Controlled Hopf Bifurcation of a Storage-Ring Free-Electron Laser

Giovanni De Ninno[1,*] and Duccio Fanelli[2,†]
[1]*Sincrotrone Trieste, 34012 Trieste, Italy*
[2]*Cell and Molecular Biology Department, Karolinska Institute, SE-171 77 Stockholm, Sweden*
(Received 2 August 2003; published 4 March 2004)

Local bifurcation control is a topic of fundamental importance in the field of nonlinear dynamical systems. We discuss an original example within the context of storage-ring free-electron laser physics by presenting a new model that enables analytical insight into the system dynamics. The transition between the stable and the unstable regimes, depending on the temporal overlapping between the light stored in the optical cavity and the electrons circulating into the ring, is found to be a Hopf bifurcation. A feedback procedure is implemented and shown to provide an effective stabilization of the unstable steady state.

DOI: 10.1103/PhysRevLett.92.094801 PACS numbers: 41.60.Cr, 29.20.Dh, 05.45.–a

Transition from stability to chaos is a common characteristic of many physical and biological systems [1,2]. Within this context, local bifurcation control is a topic of paramount importance especially for those systems in which stability is a crucial issue. This is, for example, the case for conventional and nonconventional light sources, such as storage-ring free-electron lasers (SRFELs), commonly employed in various scientific applications [3]. In a SRFEL [4], the physical mechanism responsible for light emission and amplification is the interaction between a relativistic electron beam and the magnetostatic periodic field of an undulator. Because of the effect of the magnetic field, the electrons emit synchrotron radiation, known as spontaneous emission. The light produced by the electron beam is stored in an optical cavity and amplified during successive turns of the particles in the ring. A given temporal detuning, i.e., a difference between the electron-beam revolution period and the round-trip of the photons inside the optical cavity, leads to a cumulative delay between the electrons and the laser pulses: the laser intensity may then appear as a "continuous wave (cw)" (for a weak or strong detuning) or show a stable pulsed behavior (for an intermediate detuning amount) [5,6]. The achievement of a large and stable "cw" zone is a crucial issue, of fundamental importance for experimental applications. In this Letter, we characterize the transition between stable the unstable regimes as a Hopf bifurcation. This result allows one to establish a formal bridge with the field of conventional lasers and to adopt the universal techniques of control theory to enlarge the stable signal region. We develop this idea by introducing a new model which reveals to be particularly suitable for analytic investigations. The longitudinal dynamics of a SRFEL can be described by a system of rate equations accounting for the coupled evolution of the electromagnetic field and of the longitudinal parameters of the electron bunch [7,8]. The temporal profile of the laser intensity, y_n, is updated at each pass, n, inside the optical cavity according to

$$y_{n+1}(\tau) = R^2 y_n(\tau - \epsilon)[1 + g_n(\tau)] + i_s(\tau), \qquad (1)$$

where τ is the temporal position of the electron bunch distribution with respect to the centroid; R is the mirror reflectivity; the detuning parameter ϵ is the difference between the electrons' revolution period (divided by the number of bunches) and the period of the photons inside the cavity; $i_s(\tau)$ accounts for the profile of the spontaneous emission of the optical klystron [9]. Assuming that the saturation is achieved when the peak gain is equal to the cavity losses, P, the FEL gain $g_n(\tau)$ is given by [7,8]

$$g_n(\tau) = g_i \frac{\sigma_0}{\sigma_n}\left[\frac{P\sigma_e}{g_i\sigma_0}\right]^{(\sigma_n^2-\sigma_0^2)/\gamma} \exp\left[-\frac{\tau^2}{2\sigma_{\tau,n}^2}\right], \qquad (2)$$

where g_i and σ_0 are the initial (laser-off) peak gain and beam energy spread, σ_n and $\sigma_{\tau,n}$ are the energy spread and the bunch length after the nth light-electron beam interaction, and $\gamma = \sigma_e^2 - \sigma_0^2$. Note that Eq. (2) refers to the case of SRFELs implemented on an optical klystron. The evolution of the laser-induced electron-beam energy spread is governed by the following equation:

$$\sigma_{n+1}^2 = \sigma_n^2 + \frac{2\Delta T}{\tau_s}(\gamma I_n + \sigma_0^2 - \sigma_n^2). \qquad (3)$$

Here σ_e is the equilibrium value (i.e., that reached at the laser saturation) of the energy spread at the perfect tuning, and ΔT is the bouncing period of the laser inside the optical cavity; $I_n = \int_{-\infty}^{\infty} y_n(\tau)\, d\tau$ is the laser intensity normalized to its equilibrium value (i.e., the saturation value for $\epsilon = 0$), and τ_s stands for the characteristic time of the damped oscillation of electrons in their longitudinal phase space. Equations (1)–(3) are shown to reproduce quantitatively the experimental results [8]. In particular, the laser intensity displays a stable "cw" behavior for a small amount of detuning, while a pulsed regime is found for ϵ larger than a certain critical threshold, ϵ_c. This model represents the starting point of our analysis.

Equation (1) characterizes the evolution of the statistical parameters of the laser distribution: By assuming a specific form for the profile, it is in principle possible to make explicit the evolution of each quantity. For this purpose, we put forward the assumption of a Gaussian laser profile and compute the first three moments. The details of the calculations are given elsewhere [10]. In addition, it is shown that, for ϵ spanning the central "cw" zone, the quantities $(\sigma_{l,n}/\sigma_{\tau,n})^2$ and $[(\tau_n + \epsilon)/\sigma_{\tau,n}]^2$ are small. Hence, a Taylor series expansion is performed and second order terms neglected. Finally, by approximating finite differences with differentials, the following continuous system is found:

$$\begin{cases} \frac{d\sigma}{dt} = \frac{\alpha_1}{\Delta T}\frac{1}{2\sigma}[\alpha_2 I + 1 - \sigma^2] \\ \frac{dI}{dt} = \frac{R^2 I}{\Delta T}\left[-\frac{P}{R^2} + \frac{g_i\alpha_3}{2\sigma^3}\alpha_4^{(\sigma^2-1)/\alpha_2}\left(\frac{2\sigma^2}{\alpha_3} - \sigma_l^2 - \hat{\tau}^2\right)\right] + \frac{I_s}{\Delta T} \\ \frac{d\tau}{dt} = -\frac{\tau}{\Delta T} + \frac{\hat{\tau}}{\Delta T}\left[1 - \frac{g_i}{\sigma}\alpha_3\alpha_4^{(\sigma^2-1)/\alpha_2}\frac{\sigma_l^2}{\sigma^2}\right] \\ \frac{d\sigma_l}{dt} = -\frac{1}{\Delta T}\frac{g_i}{2}\alpha_3\alpha_4^{(\sigma^2-1)/\alpha_2}\frac{\sigma_l^3}{\sigma^3} + \frac{1}{\Delta T}\frac{I_s}{I}\frac{1}{2\sigma_l}\left(\frac{\sigma^2}{\alpha_3} + \tau^2\right), \end{cases} \tag{4}$$

where $\hat{\tau} = \tau + \epsilon$ and

$$\alpha_1 = \frac{2\Delta T}{\tau_s}, \qquad \alpha_2 = \frac{\sigma_e^2 - \sigma_0^2}{\sigma_0^2}, \tag{5}$$

$$\alpha_3 = \left(\frac{\Omega}{\sigma_0\alpha}\right)^2, \qquad \alpha_4 = \frac{P\sigma_e}{g_i\sigma_0}. \tag{6}$$

Here Ω represents the oscillation frequency of the electrons in their longitudinal phase space and α, the momentum compaction factor, is a characteristic parameter of the storage ring. Note the redefinition of σ which is from here on normalized to σ_0. Although in approximate form, system (4) still captures the main features of the longitudinal SRFEL dynamics. In particular, the transition from the "cw" regime to the unstable (pulsed) steady state occurs for a temporal detuning which is close to the one found in the framework of the exact formulation, hence to the experimental value. However, system (4) fails in reproducing the correct behavior when the transition to the lateral "cw" zone is approached. In Fig. 1, phase-space portraits for both the laser intensity and the beam energy spread are plotted for different values of ϵ. Limit cycles are observed when $\epsilon > \epsilon_c$. For smaller values of ϵ, the variables converge asymptotically to a stable fixed point. The latter can be analytically characterized, thus allowing one to relate the electron-beam energy spread, intensity, centroid position, and rms value of the laser distribution, to the light-electron beam detuning. Through a stability analysis, it is also possible to determine the threshold value ϵ_c. To our knowledge, this study represents the first attempt to fully characterize the detuned SRFEL dynamics.

The fixed points $(\overline{I}, \overline{\sigma}, \overline{\tau}, \overline{\sigma}_l)$ are found by imposing $(dI)/(dt) = (d\sigma)/(dt) = (d\tau)/(dt) = (d\sigma_l)/(dt) = 0$ in (4), and solving the corresponding system. Assuming from here on that $\epsilon > 0$, then the scenario for $\epsilon < 0$ is

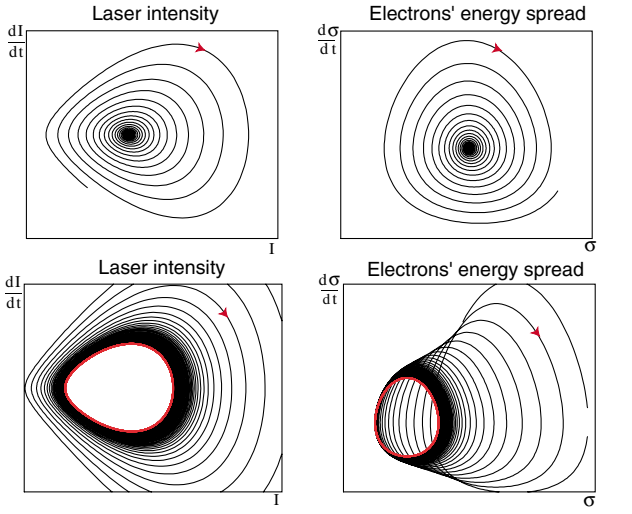

FIG. 1 (color online). Phase-space portraits. Left column: $\dot{I}$ is plotted versus I. Right column: $\dot{\sigma}$ versus σ. The top panels refer to $\epsilon = 0.1$ fs $< \epsilon_c$, the bottom ones to $\epsilon = 1.3$ fs $> \epsilon_c$. Simulations have been performed using the case of the SuperACO FEL as reference. The values of the relevant parameters are $\Delta T = 120$ ns, $\tau_s = 8.5$ ms, $\sigma_0 = 5 \times 10^{-4}$, $\sigma_e/\sigma_0 = 1.5$, $\Omega = 14$ kHz, $g_i = 2\%$, $P = 0.8\%$, and $I_s = 1.4 \times 10^{-8}$.

completely equivalent. After some algebraic calculations, the following relations are found:

$$\overline{I} = \frac{\overline{\sigma}^2 - 1}{\alpha_2}, \tag{7}$$

$$\overline{\tau} = \left\{\frac{1}{2}\left[-\frac{\overline{\sigma}^2}{\alpha_3} + \sqrt{\left(\frac{\overline{\sigma}^2}{\alpha_3}\right)^2 + 4\epsilon^2 A}\right]\right\}^{1/2}, \tag{8}$$

$$\overline{\sigma}_l = \left\{\frac{I_s}{2g_i\alpha_3}\alpha_4^{(1-\overline{\sigma}^2)/\alpha_2}\alpha_2\frac{\overline{\sigma}^3}{\overline{\sigma}^2 - 1} \times \left[\frac{\overline{\sigma}^2}{\alpha_3} + \sqrt{\left(\frac{\overline{\sigma}^2}{\alpha_3}\right)^2 + 4\epsilon^2 A}\right]\right\}^{1/4}, \tag{9}$$

where

$$A = \frac{\overline{\sigma}^3(\overline{\sigma}^2 - 1)}{\alpha_2 I_s}\frac{\alpha_4^{(1-\overline{\sigma}^2)/\alpha_2}}{g_i\alpha_3}. \tag{10}$$

These relations link the equilibrium values of $\overline{I}, \overline{\tau}, \overline{\sigma}_l$ to $\overline{\sigma}$. The quantity $\overline{\sigma}$ is found from the following implicit equation:

$$\frac{g_i}{\overline{\sigma}}\alpha_4^{(1-\overline{\sigma}^2)/\alpha_2}\left[1 - \frac{1}{2}\frac{\alpha_3}{\overline{\sigma}^2}[\overline{\sigma}_l^2 + (\overline{\tau} + \epsilon)^2]\right] = \frac{P}{R^2}, \tag{11}$$

where $\overline{\sigma}_l$ and $\overline{\tau}$ are, respectively, given by (9) and (8). For any given value of the detuning ϵ, Eq. (11) can be solved numerically, by using a standard bisection method. The estimates of $\overline{\sigma}$ are then inserted in Eqs. (7)–(9), to compute the corresponding values of $\overline{I}, \overline{\tau}, \overline{\sigma}_l$. Results of the calculations (solid line) and direct numerical simulations using the system (4) (symbols) are compared in Fig. 2, displaying remarkably good agreement. It is worth

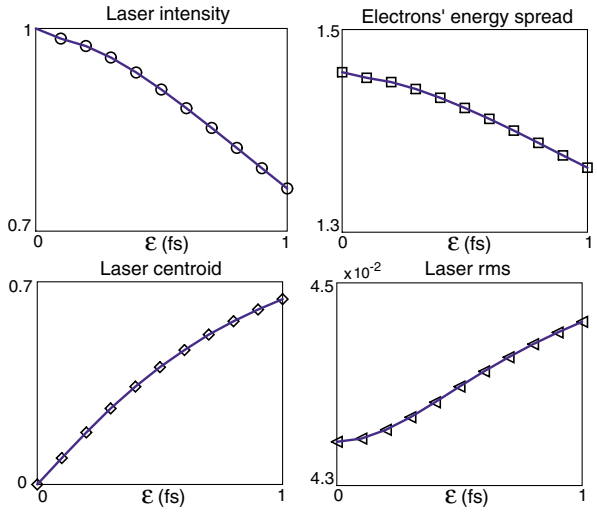

FIG. 2 (color online). The fixed points are plotted as a function of the detuning parameter ϵ. Top left panel: Normalized laser intensity. Top right panel: Normalized electron-beam energy spread. Bottom left panel: Laser centroid. Bottom right panel: rms value of the laser distribution. Symbols refer to the simulations, while the solid line stands for the analytic calculation. The list of parameters is enclosed in the caption of Fig. 1.

stressing that, by means of a perturbative analysis, a closed analytical expression for $\overline{\sigma}$ as a function of ϵ is also found. The details of the quite cumbersome calculations are given elsewhere [10].

As a validation of the preceding analysis, we consider the case of perfect tuning, i.e., $\epsilon = 0$, and compare our estimate for the laser-induced energy spread $\overline{\sigma}_l$ to the value $(\overline{\sigma}_l)_{sm}$, derived in the context of the widely used super-modes approach [11]. Both theoretical predictions are then compared to experiments performed on the SuperACO and ELETTRA FELs. Results are given in Table I: The improvement of the calculation based on Eq. (9) is clearly shown. The results of Table I indicate that both $\overline{\sigma}_l$ and $(\overline{\sigma}_l)_{sm}$ are smaller than the experimental values. This is probably due to the fact that the models neglect the effect of the microwave instability [12] resulting from the electron-beam interaction with the ring environment (e.g., the metallic wall of the vacuum chamber). In the case of ELETTRA, the situation is complicated by the presence of a "kicklike" instability (having a characteristic frequency of 50 Hz) which periodically switches off the laser preventing the attainment of a stable "cw" regime [13].

The stability of the fixed point $[\overline{I}(\epsilon), \overline{\sigma}(\epsilon), \overline{\tau}(\epsilon), \overline{\sigma}_l(\epsilon)]$ can be determined by studying the eigenvalues of the Jacobian matrix associated with the system (4). The real part of the eigenvalues as a function of ϵ is shown in Fig. 3. The system is by definition stable when all the real parts are negative. The transition to an unstable regime occurs when at least one of them becomes positive. In general, the loss of stability takes place according to different modalities. Consider the case of a Jacobian matrix with a pair of complex conjugate eigenvalues

TABLE I. Theoretical widths of the laser pulse compared to experimental values for the case of the SuperACO and ELETTRA FELs. The experimental setting for the case of SuperACO (operated at a beam energy of 800 MeV and at a laser wavelength of 350 nm) is that specified in the caption of Fig. 1. The analogous parameters for ELETTRA (operated at a beam energy of 900 MeV and at a laser wavelength of 250 nm) are the following: $\Delta T = 216$ ns, $\tau_s = 87$ ms, $\sigma_0 = 1 \times 10^{-3}$, $\sigma_e/\sigma_0 = 1.5$, $\Omega = 16$ kHz, $g_i = 15\%$, $P = 7\%$, $I_s = 4.3 \times 10^{-7}$.

	SuperACO	ELETTRA
$\overline{\sigma}_l$ (ps)	5	2
$(\overline{\sigma}_l)_{sm}$ (ps)	3	1
Experimental values (ps)	10 ± 2	5 ± 2

and assume the real parts of all the eigenvalues to be negative. A Hopf bifurcation occurs when the real part of the two complex eigenvalues becomes positive, provided the other keep their signs unchanged [14]. This situation is clearly displayed in Fig. 3, thus allowing one to conclude that the transition between the "cw" and the pulsed regime in a SRFEL is a Hopf bifurcation. The critical detuning, ϵ_c, can be calculated (open circle in Fig. 3) and displays good agreement with both the simulated data and the experimental value. A closed relation for ϵ_c is also found [10], by making use of the analytic expressions for the fixed points.

Having characterized the transition from the stable to the unstable steady state in terms of Hopf bifurcation opens up interesting perspectives to stabilize the signal and dramatically improve the system performance. In order to maintain the laser-electron beam synchronism

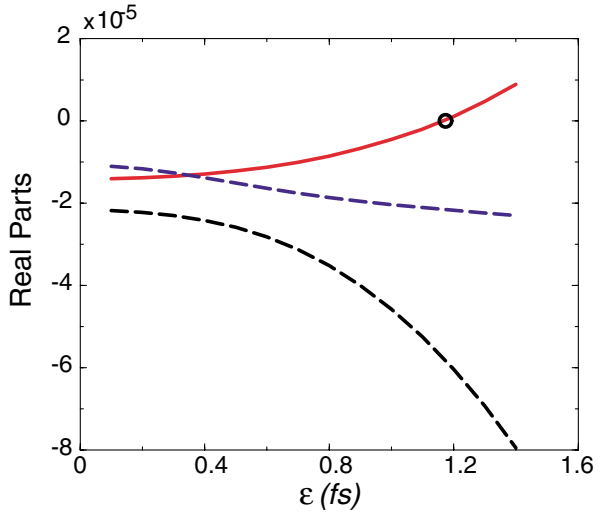

FIG. 3 (color online). Real part of the eigenvalues of the Jacobian matrix associated with the system (4) as a function of the detuning parameter ϵ. The solid line refers to the complex conjugate eigenvalues. The circle represents the transition from the stable to the pulsed regime, i.e., the Hopf bifurcation.

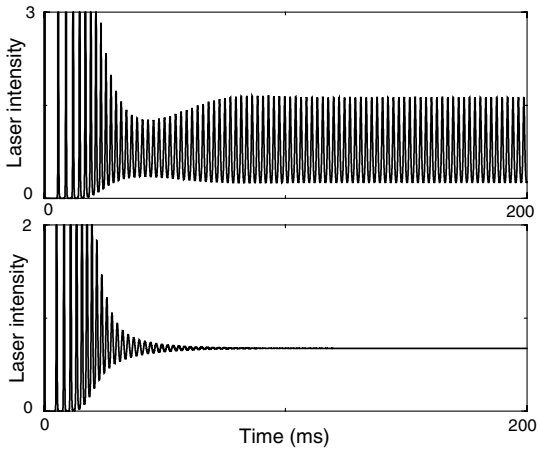

FIG. 4. Behavior of the FEL (normalized) intensity in the absence (upper panel) and in the presence (lower panel) of the derivative control system. The simulations refer to the case of SuperACO (see caption of Fig. 1 for the list of parameters). Here $\epsilon_0 = 1.3$ fs $> \epsilon_c$. The stabilization has been achieved using $\beta = 6 \times 10^{-3}$. Here, $\beta_c \simeq 5 \times 10^{-4}$.

and avoid the migration towards one of the unstable pulsed zones of the detuning curve, existing second-generation SRFELs, such as SuperACO and UVSOR [15,16], have implemented dedicated control systems. The idea is to readjust periodically the radiofrequency, thus dynamically confining the laser in the central "cw" zone. Even though generally suitable for second-generation SRFELs, these systems are inappropriate for more recent devices, such as ELETTRA and DUKE. The latters are indeed characterized by a much narrower region of stable signal only occasionally experimentally observed [13], making *a priori* impossible the pursuit of the former strategy. On the contrary, the approach discussed here exploits a *universal* property of SRFELs, thus allowing one to overcome the limitations of other schemes. The procedure consists of introducing a specific self-controlled (closed loop) feedback to suppress locally the Hopf bifurcation and *enlarge* the zone of stable signal. This is achieved by replacing the constant detuning with the time-dependent quantity [17]:

$$\epsilon(t) = \epsilon_0 + \beta \Delta T \dot{I}, \tag{12}$$

which is added to system (4). Here ϵ_0 is assumed to be larger that ϵ_c: When the control is switched off, i.e., $\beta = 0$, the laser is unstable and displays periodic oscillations. For β larger than a certain threshold, β_c, the oscillations are damped and the laser behaves as if it were in the "cw" region. Note that, as soon as saturation is reached, $\dot{I} = 0$ and, thus, the stable regime is maintained asymptotically for $\epsilon = \epsilon_0 > \epsilon_c$, i.e., well inside the former unstable zone. The results of the simulations are represented in Fig. 4.

This new theoretical insight sets the ground for experimental tests [10]. In this respect, a significant and reproducible extension of the stable "cw" region using this technique has been recently achieved at SuperACO [18]. This result fully confirms our theoretical predictions.

In conclusion, in this Letter we propose a new approximate model of a SRFEL. This formulation enables a deep analytical insight into the system dynamics, allowing one to derive the explicit dependence of the main laser parameters on the temporal detuning. Results are fully confirmed by numerical simulations and show satisfactory agreement with available experimental data. Further, the transition between the stable and unstable regimes is found to be a Hopf bifurcation, and the critical detuning ϵ_c is calculated explicitly. Finally, we introduced in the model a derivative feedback that is shown to stabilize the laser intensity well beyond the threshold ϵ_c. Successful experiments carried out at SuperACO confirmed our predictions. Preliminary experiments carried out at ELETTRA have also given encouraging results.

*Electronic address: giovanni.deninno@elettra.trieste.it
†Electronic address: duccio.fanelli@cmb.ki.se

[1] J. Guckenheimer and P. Holmes, *Nonlinear Oscillation, Dynamical Systems and Bifurcation of Vector Fields* (Springer-Verlag, Berlin, 1983).
[2] J. Keener and J. Sneyd, *Mathematical Physiology* (Springer-Verlag, New York, 1998).
[3] G. S. Edwards *et al.*, Rev. Sci. Instrum. **74**, 3207 (2003).
[4] W. B. Colson, *Laser Handbook Vol. 6* (North-Holland, Amsterdam, 1990).
[5] M. E. Couprie *et al.*, Nucl. Instrum. Methods Phys. Res., Sect. A **331**, 37 (1993).
[6] H. Hama *et al.*, Nucl. Instrum. Methods Phys. Res., Sect. A **375**, 32 (1996).
[7] M. Billardon, D. Garzella, and M. E. Couprie, Phys. Rev. Lett. **69**, 2368 (1992).
[8] G. De Ninno, D. Fanelli, C. Bruni, and M. E. Couprie, Eur. Phys. J. D **22**, 269 (2003).
[9] N. A. Vinokurov *et al.*, INP77.59, Novossibirsk, 1977.
[10] G. De Ninno and D. Fanelli, ELETTRA Technical Report No. ST/SL-03/03, 2003.
[11] G. Dattoli *et al.*, Phys. Rev. A **37**, 4326 (1988).
[12] G. Dattoli and A. Renieri, Nucl. Instrum. Methods Phys. Res., Sect. A **375**, 1 (1996).
[13] G. De Ninno *et al.*, Nucl. Instrum. Methods Phys. Res., Sect. A **507**, 274 (2003).
[14] R. C. Hilborn, *Chaos and Nonlinear Dynamics* (Oxford University Press, London, 1994).
[15] M. E. Couprie *et al.*, Nucl. Instrum. Methods Phys. Res., Sect. A **358**, 374 (1995).
[16] S. Koda *et al.*, Nucl. Instrum. Methods Phys. Res., Sect. A **475**, 211 (2001).
[17] S. Bielawski, M. Bouazaoui, and D. Derozier, Phys. Rev. A **47**, 3276 (1993).
[18] M. E. Couprie *et al.*, in Proceedings of the FEL Conference 2003 [Nucl. Instrum. Methods Phys. Res., Sect. A (to be published)].